efficacy in photodegradation of pollutants.

Thanks to the unique properties of graphene, the composite simultaneously combines three excellent properties, i.e., increasing the adsorption of pollutants, expanding the absorption range of light, and separation of charges by efficiently transferring electrons from titania to the graphene. On the other hand, some transition metal-based dyes can be used as titania sensitizers in the visible spectrum because of their high molar absorption coefficient, as well as broad absorption band [21–24]. Due to the exceptionally rigid, planar and zwitterionic structures, squaraines have strong absorption (molar absorptivity, ε, equal or more than 10^5 l.mol^{-1}.cm^{-1}) in the visible to the near-IR region. Squaraines intense absorption properties are suitable for applications related to the photosensitization phenomenon [25]. Sensitizing a TiO_2 semiconductor with squaraine may produce a highly effective photocatalytic system due to the electron transfer from the excited dye to the titania conduction band or pre-adsorbed molecular oxygen. Effective photocatalytic decomposition of different types of pollutants through dye-sensitized TiO_2 systems is due to a simultaneous effect of both semiconductor and dye. The critical factor in this cooperation is the charge transfer (e^- - h^+) as the mechanism and the type of active oxidizers produced are affected by the nature of the irradiation source. Typically, these photocatalysts are activated by irradiation with visible or sunlight, but the best efficiency for contaminant degradation is generally obtained under solar light [26].

The purpose of this work is to investigate the synergistic effect resulting from combination of a squaraine dye acting as a photosensitizer and a TiO_2/GO composite. The photocatalytic experiments were carried out under visible light irradiation in order to examine squaraine dye ability for enhancing the photoactivity of the TiO_2/rGO nanocomposite in discoloration of Methylene Blue (MB).

EXPERIMENTAL

Preparation of photocatalyst

Graphite powder (≥150 μm, ≥99.99% trace metals basis; Sigma-Aldrich), sulfuric acid (98%, Merck), sodium nitrate, potassium permanganate, and hydrogen peroxide solution (30 wt.% in H_2O) were used for the synthesis of graphene oxide. TiO_2 (Degussa, P25) and Methylene Blue (MB) were employed as ingredient for preparation of the catalyst and as substrate, respectively. The following Sigma-Aldrich chemicals were used as commercial products of analytical grade without further purification for the synthesis of squaraine dye: 1,3,3-trimethyl-2-methyleneindoline, squaric acid, and ethyl *L*-lactate.

Graphene oxide was synthesized using modified Hamer's method. The latter can be divided into three stages. The first 'cold stage' involved 5 g of graphite, 115 ml of sulfuric acid, and 2.5 g of sodium nitrate mixed in an ice bath for 30 min. Then 15 g of $KMnO_4$ were slowly added while stirring over 2 h and keeping the temperature below 5 °C since upon the reaction $KMnO_4 + H_2SO_4 = K_2SO_4 + Mn_2O_7 + H_2O$ the resulting Mn_2O_7 decomposes explosively at a temperature about 50 °C. During the second 'mid-stage', the temperature was raised to 45 °C under stirring for 1 h. Finally, 230 ml of distilled water were added, and the temperature was raised to 95 °C while stirring for 30 min. In the third 'high-temperature stage', reduction of the residual permanganate and manganese dioxide to colorless soluble manganese sulfate was achieved by adding 600 ml of distilled water and 150 ml of H_2O_2 (9%) to the mixture. The suspension was filtered, washed in 5% HCl and then in distilled water to reach neutral pH, and dried at 60 °C. The dried cake was added to 50 ml of water under stirring and then sonicated for 6 h. The dry form of graphene oxide was obtained by centrifugation, followed by drying at 60 °C [27].

TiO_2/rGO composite containing 5 wt% rGO was prepared by dissolving 10 ml of concentrated GO solution (~150 mg GO) in 500 ml if deionized (DI) water and then put under ultrasonic dispersion for about 5 h. Then 0.5 g of titania powder were gradually added into the solution to anchor the TiO_2 particles onto GO surfaces. In order to turn GO into graphene 3 g of sodium hydroxide were further added as well. After 10 h of vigorous stirring the resulting solution was transferred to a Teflon-sealed autoclave and kept under 120 °C for 24 h. Then the resulting suspension was washed with DI water, filtered, and dried at 60 °C. A reference rGO sample was prepared similarly without adding TiO_2 into the hydrothermal vessel.

For squaraine dye synthesis (Scheme 1) 1,3,3-trimethyl-2-methyleneindoline (10 mmol, 1.73 g, ~1.77 ml), squaric acid (5 mmol, 0.57 g), and ethyl L-lactate (10 ml) were placed into a 100-ml Erlenmeyer flask. The reaction mixture was heated in a microwave oven at 450 W to 140 °C. After 1 min, the reagents were dissolved and the liquid turned blue. The reaction was kept at 140 °C for 4 min. The mixture was allowed to cool down to room temperature, then diluted with ethanol (10 ml), and placed in water (200 ml) with ice (50 g). The resulting precipitate was filtered, washed with 200 ml of hot water until colorless filtrate, and finally air-dried.

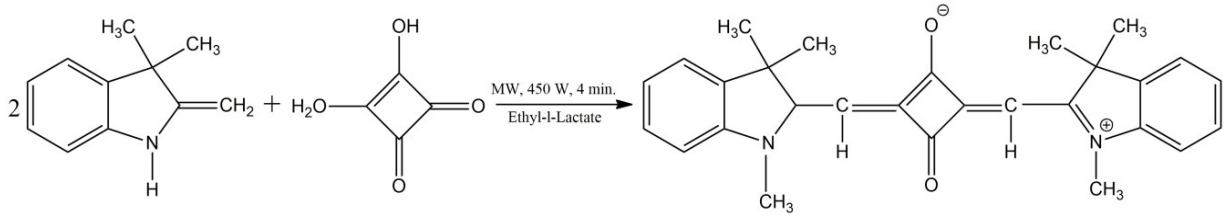

Scheme 1. Preparation of squaraine dye.

Ternary composite catalyst, TiO_2/rGO/SQ, was prepared by adding 20 mg of SQ into a 70-ml water suspension containing 60 mg of TiO_2/rGO. After continuous ultrasonication for 3 h and subsequent stirring for 2 h the resulting product was filtered and dried at 60 °C until reaching a constant mass.

Methods and experimental setup

X-ray diffraction (XRD) measurements were carried out at room temperature using a Bruker D8 Advance powder diffractometer with Cu Kα radiation source and SolX detector. The samples were scanned at 2θ angles ranging from 10° to 80° at a scanning rate of 0.04° s^{-1}.

Photocatalyst morphology was examined by a transmission electron microscope (JEOL 2100). Visible light spectra of the samples were recorded on a Shimadzu UV-2700 Vis scanning spectrophotometer.

Studies on MB photocatalytic discoloration were performed in a self-constructed cylindrical reactor (150 mm outer diameter, 130 mm high) at 25 °C, maintained by recirculating water through the reactor jacket. Photocatalytic efficiency of the catalyst was evaluated based on the degradation rate of MB (10 mg/l) in water under visible light irradiation employing a halogen lamp. A 400-ml reaction suspension containing 10 mg/l MB and 0.1 g/l catalyst was stirred for 30 min in the dark to achieve a possible adsorption-desorption equilibrium on the catalyst surface. Samples were collected at every 20 min and filtered (Whatman, Grade 42) prior to measuring absorption in the visible spectrum.

RESULTS AND DISCUSSION

Catalysts characterization

Crystalline phase composition of the prepared catalyst samples was analyzed by XRD. Fig. 1 shows the XRD patterns of the samples used in this study. The main peaks in the spectrum of the TiO_2/rGO/SQ composite catalyst correspond to tetragonal TiO_2 (anatase, 73%) dominating over rutile (23%) which was also observed in the spectrum. Comparing the XRD spectra of the individual samples presented in Fig. 1 one can see that during hydrothermal treatment as a stage of the synthesis, GO has been successfully turned into rGO. A proof of this is the disappearance of the diffraction peak at 2θ = 10.18° in the TiO_2/rGO/SQ spectrum, which is indicative of GO and its shift to 2θ = 25° characteristic of rGO [28].

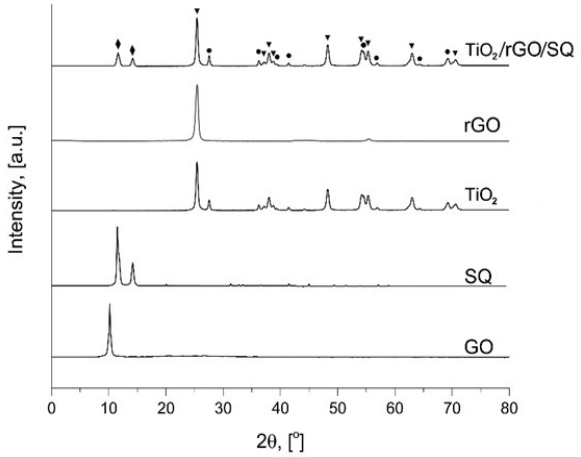

Fig. 1. XRD patterns of TiO_2 GO, SQ, rGO, and TiO_2/rGO/SQ samples (▼- anatase, ● - rutile, ♦ - SQ).

Peaks characteristic of graphene are not visible on the TiO_2/rGO/SQ composite catalyst spectrum since the main peak of rGO is at about 2θ = 25° and overlaps with that of anatase at 2θ = 25.54°. The peaks that appear on the spectrum of the ternary sample at 2θ = 11.5° and 14.2° which are specific for SQ confirmed the successful SQ attachment to the TiO_2/rGO during the catalyst synthesis. Sample morphology prior to SQ attaching was studied by high-resolution transmission electron microscopy (HRTEM) and scanning electron microscopy (SEM). Figures 2 and 3 display SEM and TEM images, respectively, of a TiO_2/rGO sample. It is seen that titania clusters are allocated on rGO sheets. Titania individual particles sizes measured from TEM images were in the range of 15–20 nm.

Photocatalytic activity testing

Titanium dioxide supported on SQ-sensitized rGO was tested for photocatalytic discoloration of MB in aqueous solution. Batch reactor experimental results were assessed in terms of maximum absorption of MB at 665 nm in the converted mixture with time under illumination. Blank experiments to evaluate MB self-destruction were also conducted.

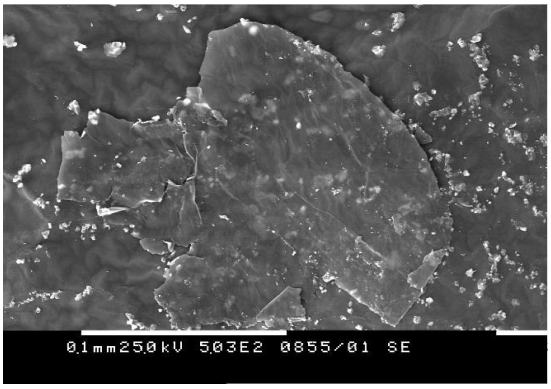

Fig. 2. SEM micrograph of TiO_2/rGO/SQ sample.

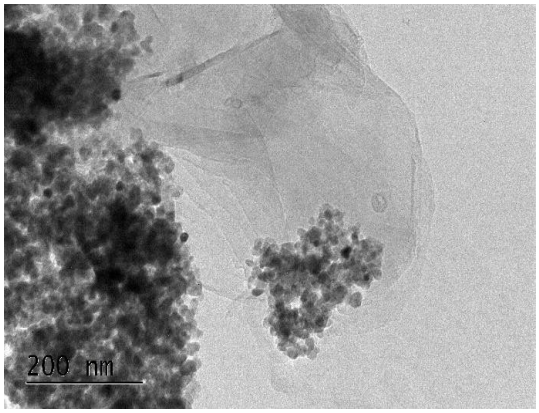

Fig. 3. TEM image of TiO_2/rGO/SQ sample.

MB concentration was calculated at equal intervals according to the absorption spectra during process applying Beer-Lambert law. The results showed that self-conversion was within the frame of 4% for 120 min of irradiation. A higher degradation efficiency concerning MB was observed using pure titania reaching ~16% conversion under the same conditions. Figure 4 discloses the absorption of the reaction solution in the course of the experiment in the presence of TiO2/rGO/SQ sample under visible light irradiation.

Discoloration efficiency (D) was evaluated applying eq. (1) to the data from Figure 5 that indicates the MB decay during illumination:

$$D\ \% = \frac{C_0 - C_t}{C_0} x100, \qquad (1)$$

where C_0 is the initial concentration of dye solution in mol/l and C_t is the concentration of dye solution after irradiation for a selected time interval in mol/l.

It was found that the nanocomposite showed a much higher degradation rate than pure titania reaching conversion over 90%, which is a remarkable photocatalytic activity under visible light illumination.

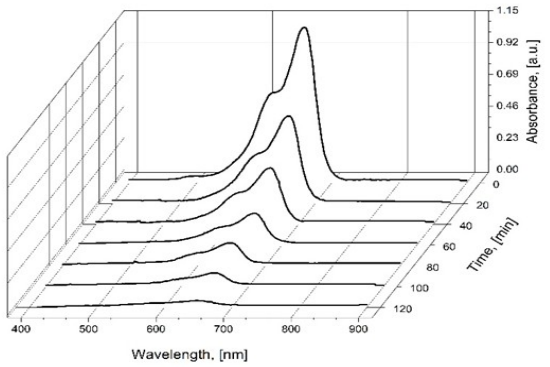

Fig. 4. Absorption spectra of MB solution during visible light irradiation.

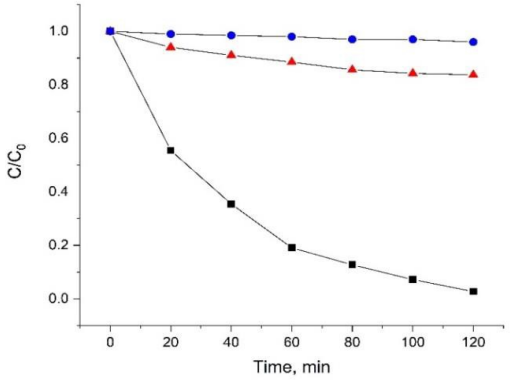

Fig. 5. Normalized discoloration curves of MB degradation under visible light in presence of: ●- self-destruction; ▲ - TiO_2; ■ - TiO_2/rGO/SQ.

A plot of *ln*[MB] versus *t* gives a straight line with coefficient of determination of 0.996 so the reaction can be considered of first order in MB. Further, using the first order kinetics we were able to calculate the apparent rate constants of MB destruction according to eq. (2):

$$ln\left(\frac{C_0}{C}\right) = k_{app}t \qquad (2)$$

or $C_t = C_0\, e^{-k_{app}t}$, where C_0 is the concentration of MB at the moment of turning on the vis-lamp and C_t is MB concentration at time *t*.

The corresponding apparent rate constants were calculated according to the plot of *ln(C0/C) versus* time (Fig. 6). The highest rate constant reaching a value of 0.028 mol/l.s was exhibited in the presence of TiO_2/rGO/SQ composite catalyst that was 18 times higher than that over bare titania.

As titania has a wide energy band gap of 3.2 eV and remains transparent to the visible light, its photonic efficiency is close to zero because of the insufficient photon energy needed for excitation of the electrons from the valence to the conduction band.

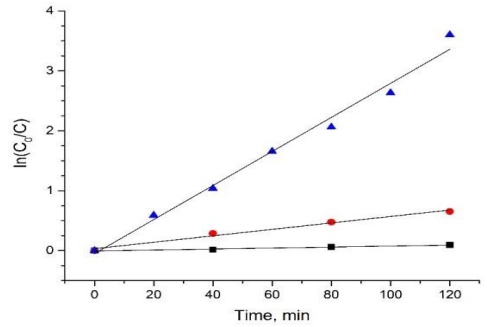

Fig. 6. Apparent rate constants of MB degradation under Vis-light (▲ - TiO_2/rGO/SQ; ● - TiO_2; ■ - self-destruction).

In this case, photodegradation of the dye is realized by a photosensitization procedure as the light is almost exclusively absorbed by the dye with subsequent transfer of the excited electron into the conduction band of the semiconductor leaving behind a hole localized on the dye. Then the atmospheric molecular oxygen acts as a scavenger for the separated electron so that the recombination of the e^-/h^+ is being prevented and the dye is destroyed by the remaining hole [29]. Photodegradation by direct excitation of titania is not excluded but it is very limited. Having investigated TiO_2 and graphene as photocatalysts for MB degradation, Markad *et al.* [30] confirmed that there is an insignificant change in concentration of MB after illumination for sufficiently long time indicating inability of these materials to act as a photocatalyst individually in visible light. The self-destruction rate could be neglected because it takes place at a much lower rate constant estimated to be 8.24×10^{-4} mol/l.s. Further, the MB discoloration was studied by incorporating graphene and SQ in the titania to investigate the synergic effect of coupling these materials.

The combination of rGO and SQ together with TiO_2 was found to be the most effective MB destroyer, having an apparent rate constant of 0.028 mol/l.s as mentioned above. This result was achieved as each of these three components gives its contribution to the overall decomposition process shown in Figure 7.

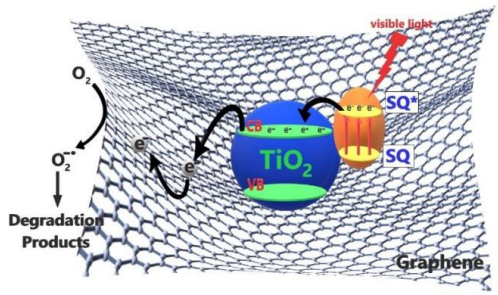

Fig. 7. Schematic illustration of the MB destruction mechanism.

CONCLUSION

A ternary squaraine photosensitized titania catalyst containing 5 wt% reduced graphene oxide was synthesized. The novel TiO_2/rGO/SQ catalyst exhibited a remarkable activity with respect to MB photodiscoloration in aqueous solution under visible light irradiation leading to increasing the apparent rate constant of the process by 18 times compared to that of bare titania.

Acknowledgement: *The authors gratefully acknowledge financial support by Bulgarian National Science Fund, Ministry of Education and Science of Bulgaria (Project DFNI 239/28.02.2019).*

REFERENCES

1. T. Suzuki, S. Tinolei, L. Kurunczi, U. Dietze, G. Schuuirmann, *Chemosphere*, **45**, 1 (2001).
2. F. D. Ollis, E. Pelizzetti, N. Serpone, in: Photocatalysis: Fundamentals and Applications, N. Serpone and E. Pelizzetti (eds.), Wiley Interscience, New York, 1989, p. 603.
3. R. M. Hoffmann, S. T. Martin, W. Choi, D. W. Bahnemannt, *Chem. Rev.*, **95**, 69 (1995).
4. C. M. Yeber, J. Rodríguez, J. Freer, N. D. Durán, H. Mansilla, *Chemosphere*, **41**, 1193 (2000).
5. J. M. Herrmann, *Topics Catal.*, **34**, 49 (2005)
6. G. P. Anipsitakis, D. D. Dionysiou., *Appl. Catal. B: Environ.*, **54**, 155 (2004).
7. A. Matilainen, M. Sillanpää., *Chemosphere*, **80**, 351 (2010).
8. J. M. Monteagudo, A. Durán, I. San Martín, *J. Environ. Manage*, **141**, 61 (2014).
9. X. Huang, B. Feng, Y. Niu, *Catal. Lett.*, **148**, 1 (2018).
10. S. Anandan, Y. Ikuma, K. Niwa., *Solid State Phenom.*, **162**, 239 (2010).
11. H. Lin, C. P. Huang, W. Li, C. Ni, I. Shah, Y.-H. Tseng, *Appl. Catal. B: Environ.*, **68**, 1 (2006).
12. K. Rajeshwar, M. E. Osugi, W. Chanmanee, C. R. Chenthamarakshan, *J. Photochem. Photobiol. C: Photochem. Rev.*, **9**, 172 (2008).
13. V. Subramanian, E. Wolf, P. V. Kamat, *J. Phys. Chem. B*, **105**, 11439 (2001).
14. A. Sclafania, J. Herrmann, *J. Photochem. Photobiol.*, **113**, 181 (1998).
15. K. Venkata, S. Rao, B. Lavédrine, P. Boule, *J. Photochem. Photobiol. A: Chem.*, **154**, 189 (2003).
16. B. Yao, C. Peng, W. Zhang, Q. Zhang, J. Niu, J. Zhao, *Appl. Catal. B: Environ.*, **174-175**, 77 (2015).
17. C. Wang, J. Li, G. Mele, G. M. Yang, F. X. Zhang, L. Palmisano, G. Vasapollo, *Appl. Catal. B: Environ.*, **76**, 218 (2007).
18. K. Assaker, C. Carteret, T. Roques-Carmes, J. Ghanbaja, M. J. Stébéa, J. L. Blin, *New J. Chem.*, **38**, 208 (2014).
19. T. Batakliev, I. Petrova-Doycheva, V. Angelov, V. Georgiev, E. Ivanov, R. Kotsilkova, M. Casa, C.

Cirillo, R. Adami, M. Sarno, P. Ciambelli, *Appl. Sci.*, **9**, 469 (2019).
20. G. Spinelli, P. Lamberti, V. Tucci, R. Kotsilkova, S. Tabakova, R. Ivanova, P. Angelova, V. Angelov, E. Ivanov, R. D. Maio, C. Silvestre, D. Meisak, A Paddubskaya, P. Kushir, *Materials*, **11**, 2256 (2018).
21. A. Kruth, S. Peglow, N. Rockstroh, H. Junge, V. Brüser, K. D. Weltmann, *J. Photochem. Photobiol. A: Chem.*, **290**, 31 (2014).
22. Z. S. Seddigi, S. A. Ahmed, S. Sardar, S. K. Pal, *Photochem. Photobiol. Sci.*, **15**, 920 (2016).
23. D. J. Wasylenko, R. D. Palmer, E. Schott, C. P. Berlinguette, *Chem. Commun.*, **48**, 2107 (2012).
24. E. Regulska, D. Rivera-Nazario, J. Karpinska, M. Planska-Brzezinska, L. Echegoyen, *Molecules*, **24**, 1118 (2019).
25. S. Minkovska, N. Burdzhiev, A. Alexiev, T. Deligeorgiev, *Chem. Papers*, **72**, 1549 (2018).
26. Z. Youssef, L. Colombeau, N. Yesmurzayeva, F. Baros, R. Vanderesse, T. Hamieh, J. Toufaily, C. Frochot, T. Roques-Carmes, S. Acherar, *Dyes Pigm.*, **159**, 49 (2018).
27. S. Alam, N. Sharma, L. Kumar, *Graphene*, **6**, 1 (2017).
28. L. Stobinski, B. Lesiak, A. Malolepszy, M. Mazurkiewicz, B. Mierzwa, J. Zemek, P. Jiricek, I. Bieloshapka, *J. Electron Spectrosc. Relat. Phenom.*, **195**, 145 (2014).
29. E. Stathatos, T. Petrova, P. Lianos, *Langmuir*, **17**, 5025 (2001).
30. G. Markad, S. Kapoor, S. Haram, P. Thakur, *Solar Energy*, **144**, 127 (2017).